



ISSN: 0067-2904

DC Sputtering Deposition of Copper Oxide Thin Films Doped with Carbon for Efficient Solar Selective Absorbers

Sawsan H. Abdullah¹, Hammad R. Humud², Falah. I. Mustafa²

¹Department of Physics, College of Science, University of Baghdad, Iraq

²Ministry of Science and Technology, Iraq,

Received: 11/7/2021

Accepted: 6/11/2021

Published: 30/7/2022

Abstract

In this work, carbon-doped copper oxide thin films were deposited by the reactive DC sputtering method for use as selective absorbers. The properties of the DC discharge plasma were studied, using the emission spectrum, in the presence of pure argon and by mixing it with oxygen once and carbon dioxide again to know the effect of adding these gases on the properties of the resulting plasma used in the deposition of films. The structural properties of the deposited thin films prepared with different flow ratio of carbon dioxide gas were studied using x-ray diffraction. To examine the selective absorber coatings, the reflectance within the UV-Vis spectrum was measured to calculate the percentage of energy absorbed by solar radiation using numerical integration. The reflectance was also measured in the range from 2.5 to 25 μm to calculate the thermal emission of the solar heater within a temperature of 373 K. Measurements showed good efficiency as a selective absorption layer. The best absorptance of the solar spectrum (α) was 0.8750, and the lowest emittance (ϵ) in the infrared region was 0.254 at 25% percentage of carbon dioxide in the reactive gas of the sputtering system. So, this ratio has the highest efficiency as a selective absorber.

Keywords: CuO: C thin films, DC sputtering, selective absorber.

ترسيب التريز بالتيار المستمر لأغشية رقيقة من أكسيد النحاس المشوبة بالكربون كماص انتقائي فعال للطاقة الشمسية

سوسن حسين عبد الله^{1*} ، حمد رحيم حمود¹ ، فلاح ابراهيم مصطفى²

¹قسم الفيزياء ، كلية العلوم ، جامعة بغداد ، بغداد ، العراق

²وزارة العلوم والتكنولوجيا ، بغداد ، العراق

الخلاصة

تم في هذا العمل ترسيب أغشية رقيقة من أكسيد النحاس المشوب بالكربون بواسطة طريقة التريز بالتيار المستمر التفاعلية لاستخدامها كمتصات انتقائية. تمت دراسة خواص بلازما التفريغ المستمر باستخدام طيف الانبعاث بوجود الأرجون النقي ثم مزجها مع الأكسجين مرة ومرة ثانية أكسيد الكربون مرة أخرى لمعرفة تأثير إضافة هذه الغازات على خواص البلازما الناتجة المستخدمة في ترسيب الأغشية. تمت دراسة الخواص التركيبية للأغشية الرقيقة المحضرة بنسب تدفق مختلفة لغاز ثاني أكسيد الكربون. لفحص الطلاءات الماصة الانتقائية ، تم قياس الانعكاسية ضمن الطيف فوق بنفسجي- مرئي لحساب النسبة المئوية للطاقة التي

*Email: Sawsanhussein1976@gmail.com

يتمتعها الإشعاع الشمسي باستخدام التكامل العددي. تم قياس الانعكاس أيضًا في المدى من 2.5 إلى 25 ميكرومتر لحساب الانبعاث الحراري للسخان الشمسي في درجة حرارة 373 كلفن. أظهرت القياسات كفاءة جيدة كطبقة امتصاص انتقائية. أفضل امتصاصية للطيف الشمسي (α) كانت 0.8750، وأقل انبعاثية (ϵ) في منطقة الأشعة تحت الحمراء كانت 0.254 عند نسبة ثاني أكسيد الكربون 25% من الغاز المتفاعل في منظومة التريذيد. لذلك، هذه النسبة لها أعلى كفاءة كمتص انتقائي.

1. Introduction

Because of the global importance of energy and the necessity to reduce pollution and greenhouse gases problems, the need for new alternatives of renewable energies has emerged, including the use of solar energy [1]. The exploitation of solar energy through direct heat absorption by solar collectors is one of the simple and highly efficient methods [2]. Selective absorber coatings have a high absorption of solar radiation in the UV-Visible spectrum as well as low emittance at the operating temperature, which is usually in the infrared region [3]. Despite the high absorbance of solar black coatings, it cannot be considered a selective surface due to its high infrared emissivity [4]. To obtain good selective surfaces, a mixture of different materials is used such as grafting metal oxides with carbon [5].

The selective absorber efficiency is determined by its total absorbance of solar energy by a layer on a metal panel. It is usually calculated using the reflectivity curve and the standard solar spectrum at sea level from calculating the ratio between the entire absorbed energy to the total falling energy, which is calculated from the area under the solar radiation curve. While the emittance at the infrared region is calculated using Kirchhoff's laws [6], using the reflectance spectrum within the blackbody emission range of the proposed operating temperature of the solar absorber [7].

Plasma sputtering using DC discharge is one of the thin film deposition methods that produces thin films with uniform coating and with high-quality specifications. It is important to study the plasma parameters to control the sputtering process and to know their effect on the properties of the deposited films. Plasma emission spectrometry is one of the methods used to study plasma properties. Plasma emission spectrum consists of several spectral lines describing electronic transitions in an atom or ion [8]. The intensity of the spectral lines varies depending on the plasma temperature, the quantitative transition probability and the statistical weight of the excited plane, as in the Boltzmann distribution equation [9]:

$$I_{ji} = \frac{N}{U(T)} g_j A_{ji} h\nu_{ji} e^{-E_j/k_B T_e} \quad (1)$$

Where: g_j represents the upper-level statistical weight, E_j is the upper-level energy, A_{ji} represents the transition probability and T_e is the plasma temperature represented by the electron temperature, which can be calculated using Boltzmann relationship [10]:

$$\ln \left(\frac{I_{ji} \lambda_{ji}}{g_j A_{ji}} \right) = \left(-\frac{E_j}{k T_e} \right) + \left(\frac{N(T)}{U(T)} \right) \quad (2)$$

Where λ_{ji} is the wavelength generated by the transition from the j level to the i lower level.

Whereas, the electron density can be calculated, using the Stark expansion relationship [11]

$$n_e (cm^{-3}) = \left[\frac{\Delta\lambda}{2\omega_s(\lambda, T_e)} \right] N_r \quad (3)$$

Where: $\Delta\lambda$ is the width of the spectral line at the mid-intensity, and ω_s is the electron effect parameter, which can be found from the standard tables, and N_r is the reference electron density equal to $10^{16} cm^{-3}$ for atoms and $10^{17} cm^{-3}$ for ions.

In this research, the effect of mixing ratios of carbon dioxide and oxygen with argon, as a mixture of reacting gases in a DC discharge sputtering system, on the properties of the deposited films was studied. In addition, the properties of the carbon-doped copper oxide deposited films, such as the structural properties, was studied. The effect of the gas mixing

ratio, which changes the percentage of doping with carbon, on the efficiency of films deposited on a copper substrate as selective absorbers was also studied.

2. Experimental

A copper target, of a purity greater than 99 %, was used to prepare the DC discharge target. The reactive gases Ar, O₂, and CO₂ were to flow in the discharge chamber with three different ratios of Ar:O₂:CO₂: (70:10:20, 65:10:25, and 60:10:30) percentage., The deposition parameters were 1300 V sputtering voltage, 25 mA current, 8×10^{-2} mbar pressure, and 3.6 cm inter-electrode distance.

Glass and copper substrates were used with an area of 2×2.5 cm². The copper substrates were polished by three stages, finally cleaned with ethanol in ultrasonic water bath for 10 minutes and dried with an air blower.

Plasma characteristics were studied using plasma emission spectroscopy. The emission, produced by the reactive DC discharge using different gasses (Ar, Ar: O₂ =70:30, and Ar: CO₂ =70:30), was transferred, by optical fibre, to a spectrometer to be analysed. The spectrometer was connected with a computer to record the data, which were then used to study the effect of the gas mixture on the properties of DC discharge plasma.

The deposited thin films prepared at different mixing ratios of the different CO₂ ratios ,as the reactive gas, with oxygen and argon were examined by the XRD measurements. To examine the selective absorber efficiency, the reflectance patterns of the prepared thin films were registered with a reflection spectroscope (Avantes DH-S-BAL-2048 UV-Vis), within the range of 200 to 1100 nm. The thin films were also examined using Fourier transform infrared spectroscopy with a reflection mode (FTIR Bruker ALPHA II Spectrophotometer) at the range of 2.5 to 25 μ m.

3. Results and Discussions

3.1 Plasma Characterization

Figure1 shows the spectroscopic emission patterns of the plasma produced by DC sputtering in Ar gas at 2×10^{-1} mbar pressure using copper target which were compared with the standard lines for (Ar I, Ar II, and Cu I) [12]. There are many atomic and ionic argon lines, in addition to weak lines for Cu from the sputtered atoms, which has low concentration compared with argon atoms. The peaks intensities of Ar I atomic lines are much higher than those the ArII ionic lines (ArII) indicating the partial ionization of argon gas.

Figure 2 shows the spectroscopic emission patterns of the plasma produced by DC sputtering at mixed gasses of Ar and CO₂ gas at 2×10^{-1} mbar pressure using copper target compared with the standard lines. There are many atomic and ionic argon lines, in addition to weak lines for Cu. A small peak appeared at 777.6 nm corresponding to OI [13]. Additional broad peaks appeared at 389.3 and 426 nm corresponding to molecular bands for CO and CO₂, respectively. These peaks are from the difference in electronic and vibrational energy levels of the two molecules.

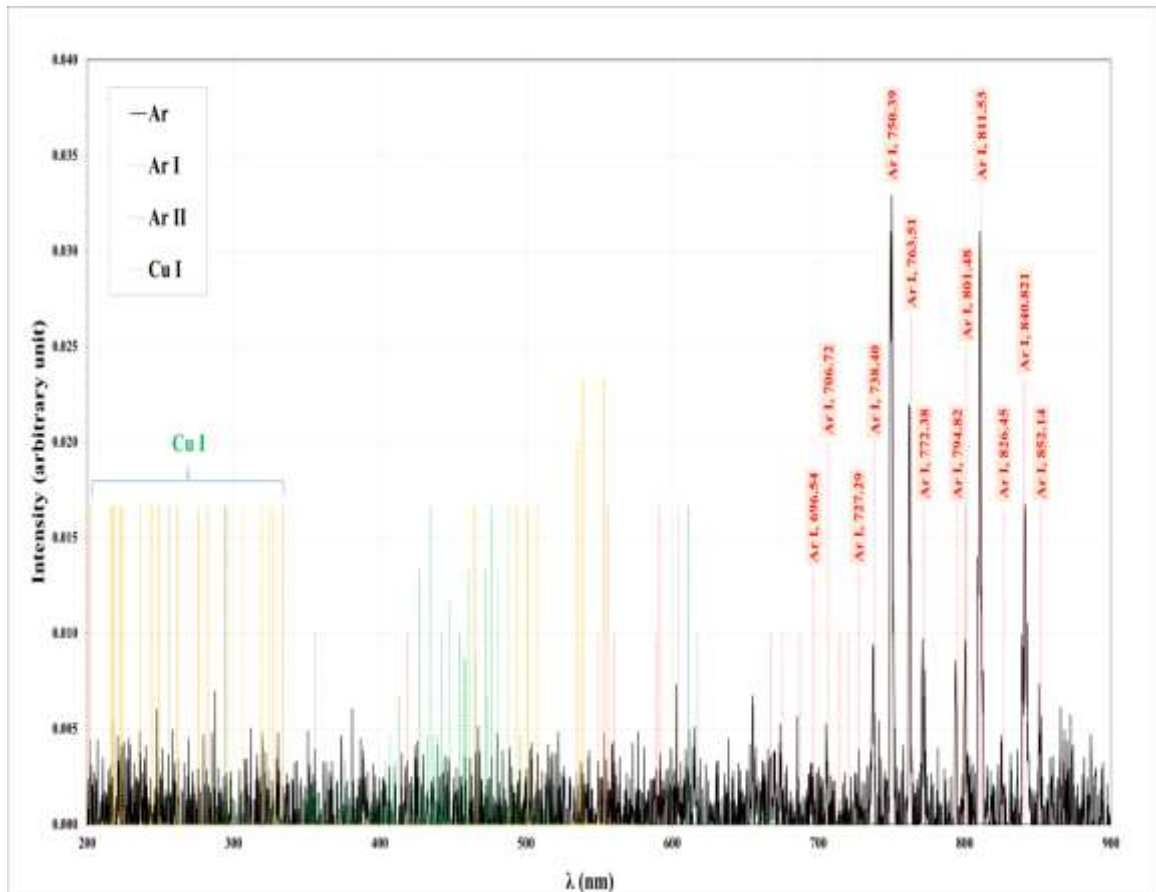


Figure 1- Emission spectrum for DC sputtering in Ar gas using copper target.

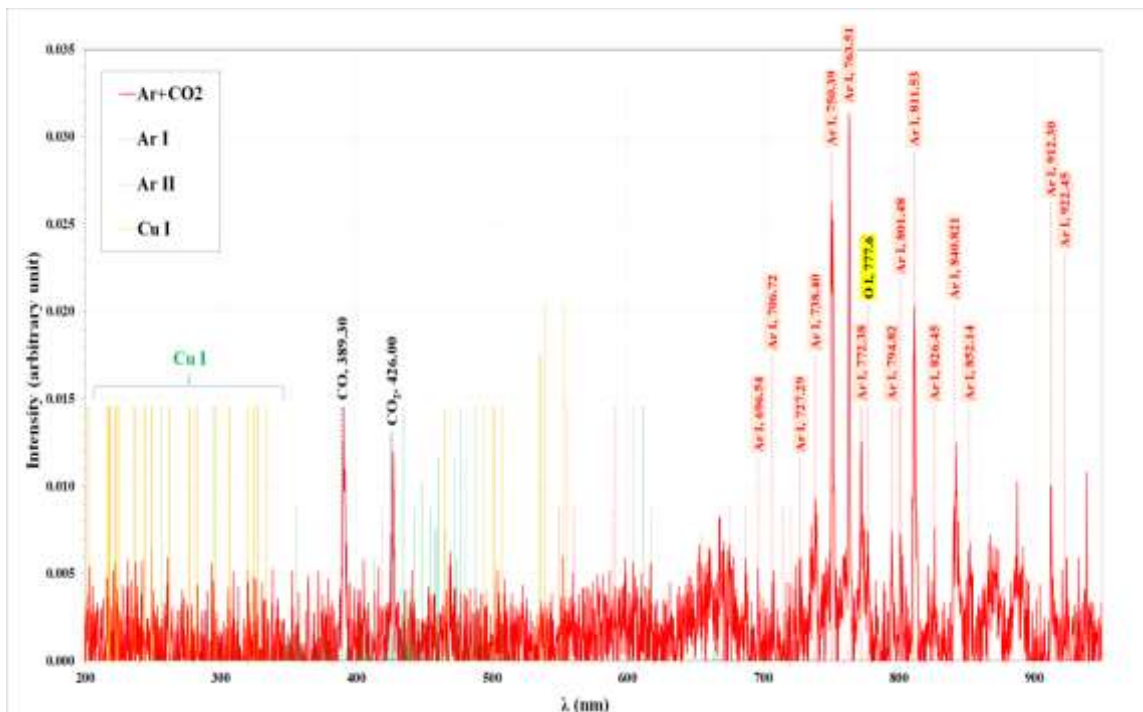


Figure 2- Emission spectrum for DC sputtering in Ar mixed with CO₂ gas using copper target.

Figure 3 shows the spectroscopic emission patterns of the plasma produced by DC sputtering in mixed gasses of Ar and O₂ gas at 2×10^{-1} mbar pressure using copper target. The same

atomic and ionic argon lines and small intensities Cu line were noticed. The evidence peak appeared at 777.6 nm corresponding to O I for oxygen gas.

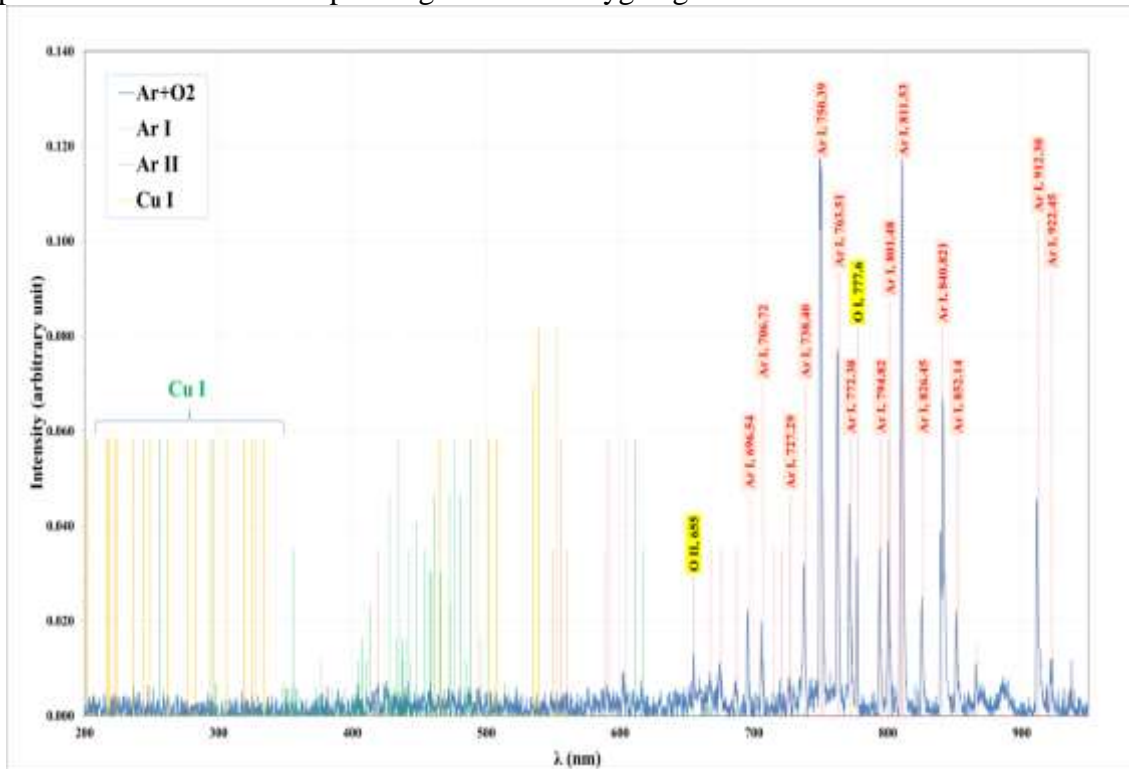


Figure 3-Emission spectrum for DC sputtering in Ar mixed with O₂ gas using copper target.

Figure 4 shows the peak profile for the Ar line at 763.51 nm for the emission from DC sputtering in the three different gasses (Ar, Ar+CO₂, and Ar+O₂). The full width at half maximum was found by Lorentzian fitting which was used to calculate electron density for the different samples using the previously calculated standard broadening for this line [14].

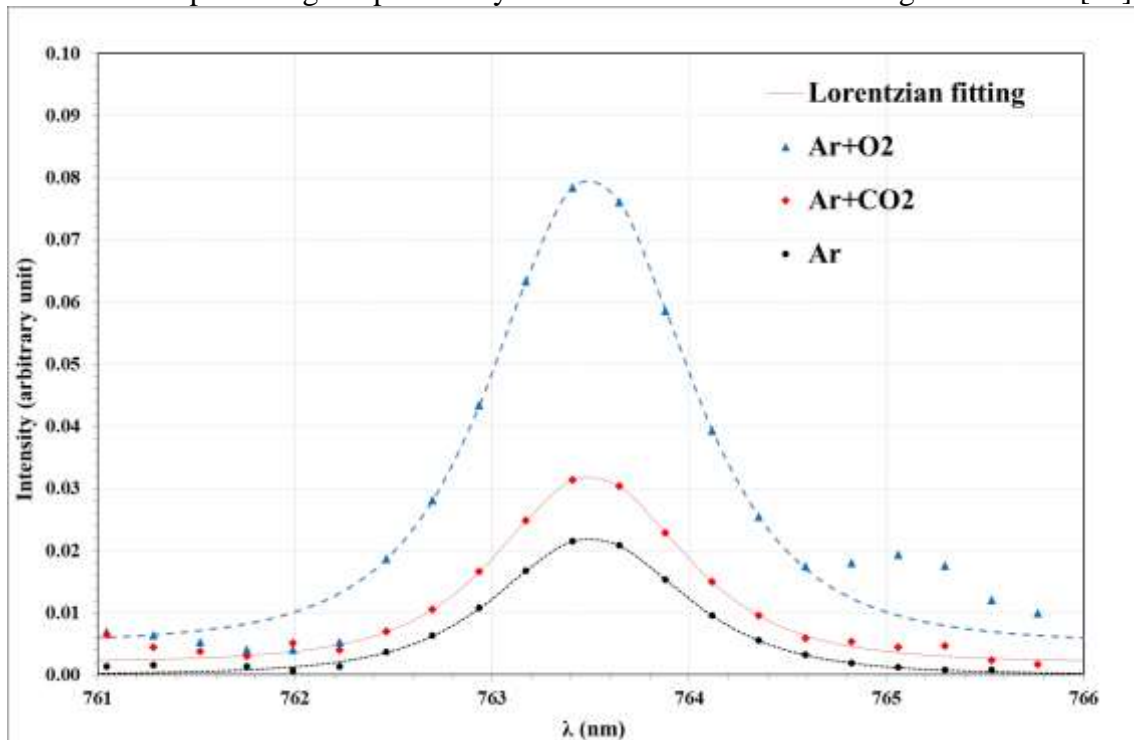


Figure 4-Lines profile and their Lorentzian fitting for ArI line at 763.5 nm from DC sputtering in different gas mixtures.

Electron temperatures (T_e) were calculated from the slope of the relation between $\ln\left(\frac{I_{ji}\lambda_{ji}}{hc g_j A_{ji}}\right)$ versus upper energy level, using Boltzmann plot method[15], as shown in Figure 5, for the atomic lines of argon emission lines from DC sputtering in the different gasses mixtures.

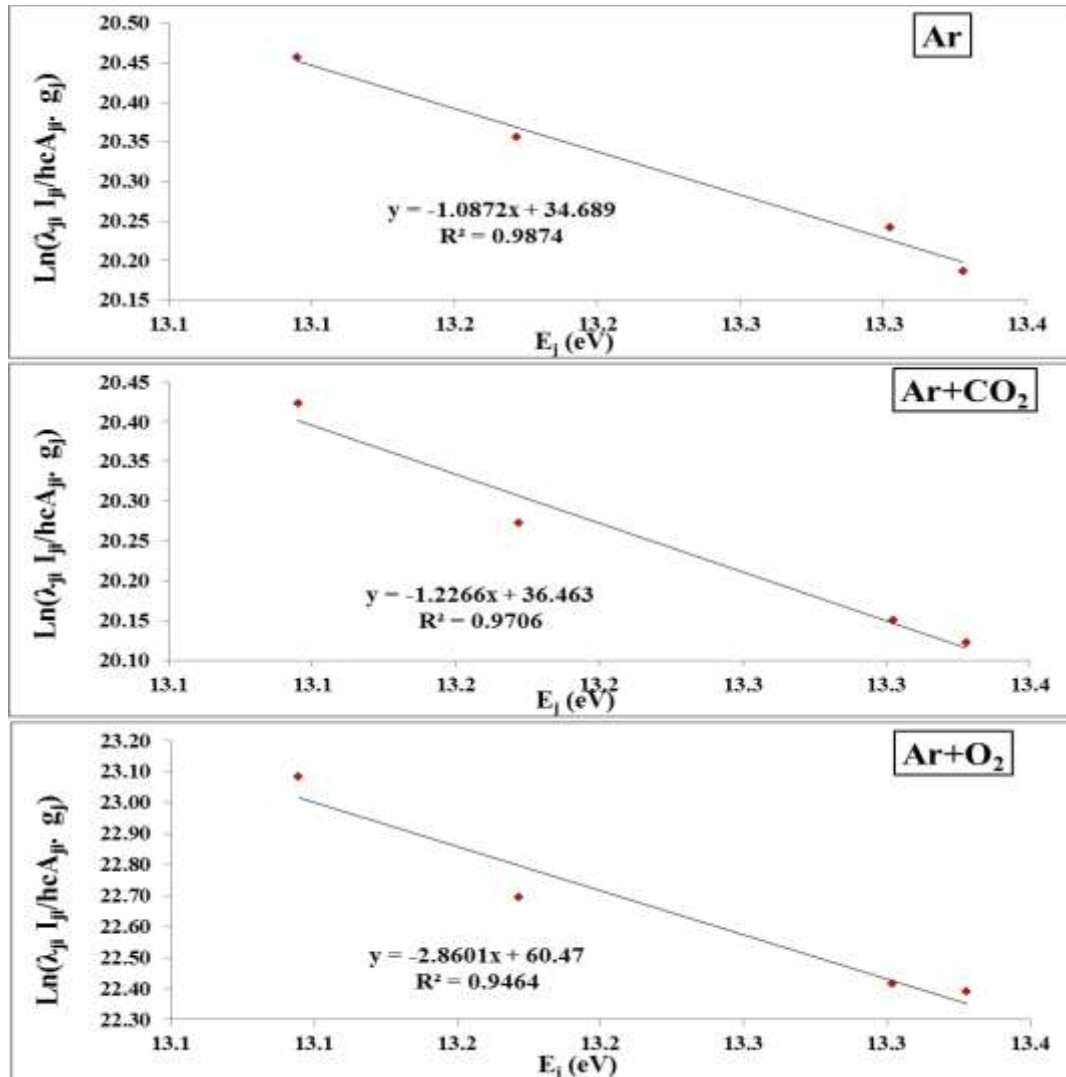


Figure 5-Boltzmann plots using ArI lines produced by DC sputtering in Ar, Ar+CO₂, and Ar+O₂ mixed gasses.

Table 1 shows the calculated parameters of the plasma produced by DC sputtering in the different gasses. The plasma temperature (T_e) decreases by adding carbon dioxide gas to argon with the ratio of 30%, and decreases further by adding oxygen at the same ratio. This decrease in temperature occurs because not all the energy supplied to the gas mixture, which contains molecular gases, goes to the electrons. Part of the energy is in the form of vibrational energy or rotational energy of these molecules. On the other hand, the electron density changed slightly.

Table 1-plasma parameters calculated from spectroscopy lines for DC sputtering in different gasses.

Sample	T_e (eV)	FWHM (nm)	$n_{e \times 10^{17}}$ (cm ⁻³)	$f_p(\text{Hz}) \times 10^{12}$	$\lambda_D \times 10^{-6}$ (cm)
Ar	0.920	1.120	7.568	7.812	0.819
Ar+CO ₂	0.815	1.100	7.432	7.742	0.778
Ar+O ₂	0.350	1.150	7.770	7.916	0.498

3.2 Thin films Characterization

The prepared thin films were uniformly deposited and had very high adhesion, it was difficult to remove by scratching, which makes them resistant to environmental conditions. The colours of the prepared films varied from brown to dark brown with the increasing percentage of carbon in the sample.

Figure 6 displays the X-ray diffraction patterns of the C-doped CuO thin films deposited on glass substrates by the DC sputtering using the different mix ratios of gases (20%, 25% and 30% CO₂). Poly-crystalline structure of monoclinic copper oxide structure appeared in all samples (standard card No. 96-101-1195) with peaks located at 32.5626°, 35.3531°, and 38.4624° compared with the lattice planes of (110), (11-1), and (111), respectively. Additional peak appeared with 25% CO₂ gas located at 26.66° corresponding to (002) direction of hexagonal graphite structure, matched with standard card No. 96-901-2231. The intensity of this peak increased with increasing the CO₂ gas flow to 30% indicating the increase of the carbon content in the sample [16].

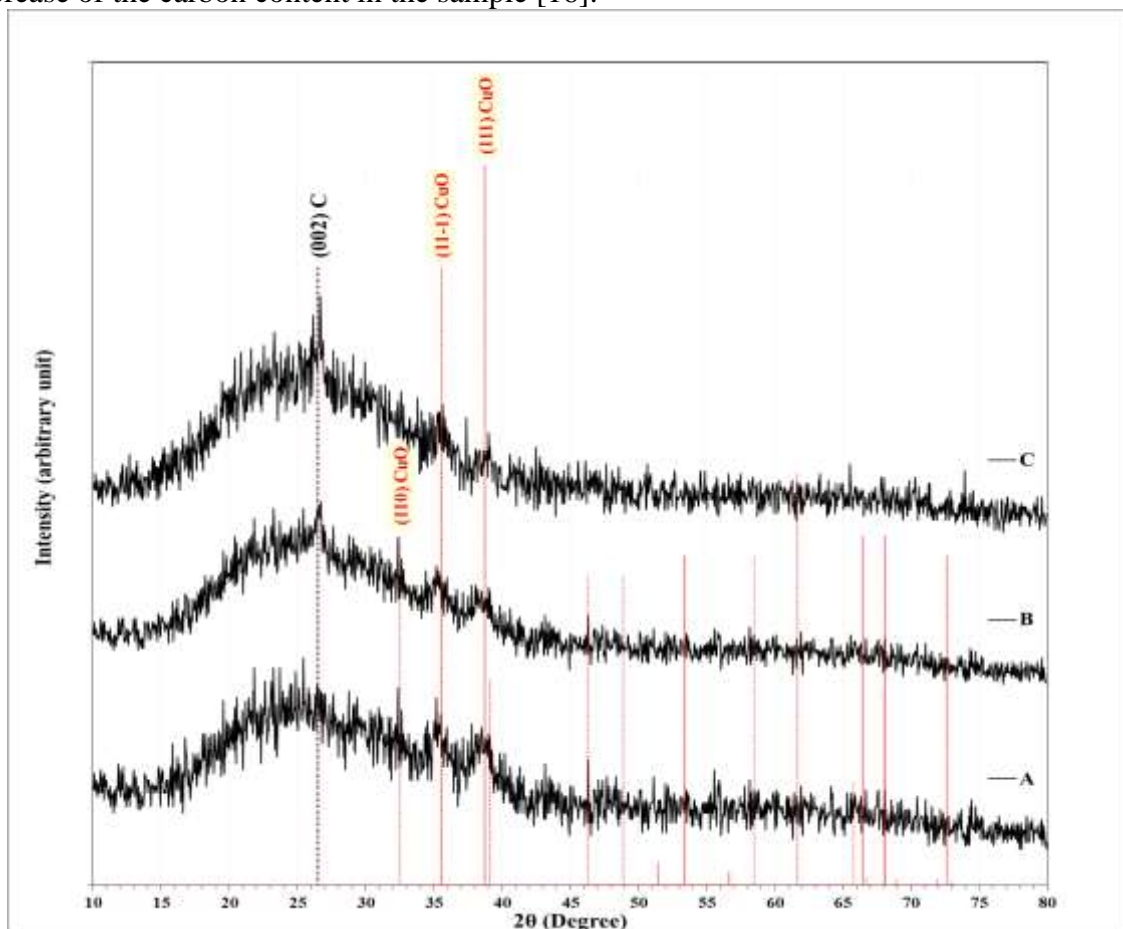


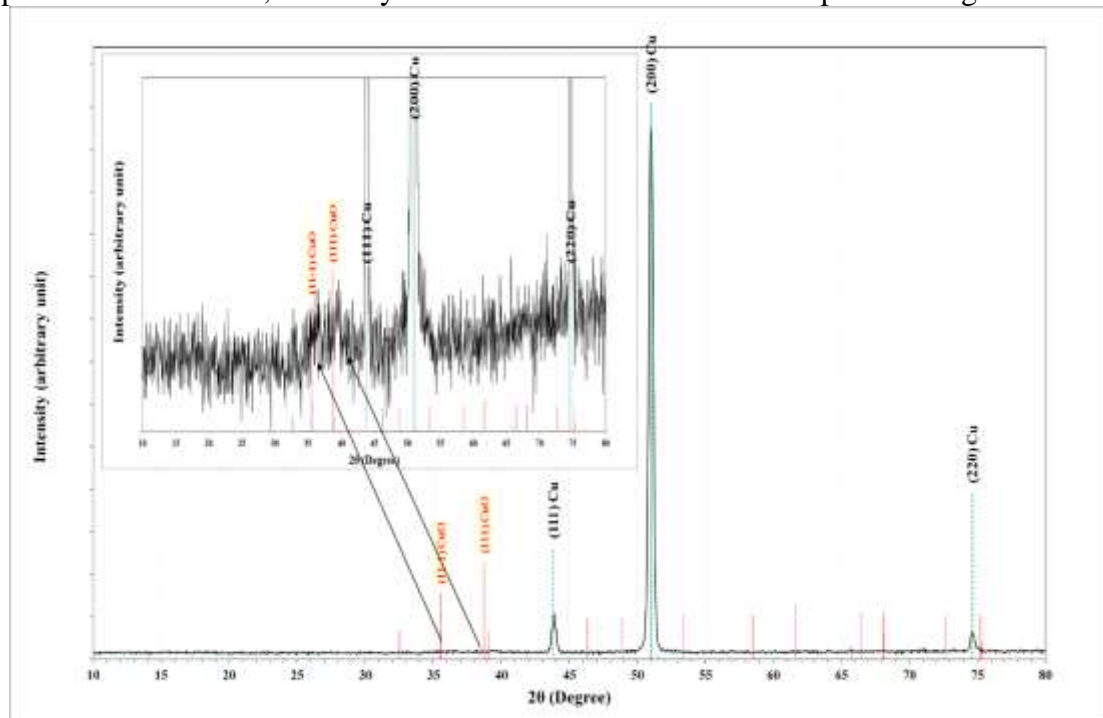
Figure 6-X-ray diffraction patterns for CuO:C thin film deposited on glass substrate by DC sputtering at different CO₂ mixing ratios of (A) 20%, (B) 25 and, (C) 30% with the Ar and O₂ gasses.

Table 2 shows the diffraction angles, inter-planer spacing (d_{hkl}) calculated using Bragg's law, full width at half maxima (FWHM), crystalline size (C.S.), and corresponding Miller indices for the XRD peaks in the three samples. There is a slight change in the diffraction angles due to lattice stresses arising because of crystal defects due to doping. The table also shows that the crystal size values of copper oxide did not change much, while the crystalline size of carbon increased significantly when the percentage of carbon dioxide increased from 25 to 30%.

Table 2- XRD parameters for CuO: C thin film deposited on glass substrates prepared by DC sputtering using different CO₂ mixing ratios.

CO ₂ %	2θ (Deg.)	FWHM (Deg.)	d _{hkl} (Å)	C.S (nm)	hkl	Phase
20	32.5626	1.1161	2.7476	7.4	(110)	Mono.CuO
	35.3531	1.0364	2.5369	8.0	(11-1)	Mono.CuO
	38.4624	1.3553	2.3386	6.2	(111)	Mono.CuO
	26.6629	0.5581	3.3406	14.6	(002)	Graphite
25	32.4032	0.7175	2.7608	11.5	(110)	Mono.CuO
	35.2733	1.1162	2.5424	7.5	(11-1)	Mono.CuO
	38.3827	1.1959	2.3433	7.0	(111)	Mono.CuO
	26.6629	0.7176	3.3406	11.4	(002)	Graphite
30	35.4328	1.0364	2.5313	8.1	(11-1)	Mono.CuO
	39.0205	0.9568	2.3065	8.8	(111)	Mono.CuO

Figure 7 shows the X-ray diffraction patterns of C-doped CuO thin films deposited on a copper substrate using a gaseous mixture containing 25% carbon dioxide. From the figure, it is noticed that the peaks of copper substrate overshadowed the figure, so it was difficult to notice the peaks belonging to the deposited films. To focus on the copper oxide peaks, the figure was scaled up as shown in the inset figure, which shows small peaks belonging to the copper oxide. Therefore, the analysis was sufficient for the films deposited on glass.

**Figure 7-**XRD parameters for CuO: C thin film deposited on Cu substrate prepared by DC sputtering.

3.3 Selective Absorber Examination

The comparison between the standard solar irradiance curve (AM 1.5 Standard Spectrum) and the absorbed energy for the Cu substrate coated with C: CuO thin films prepared by DC sputtering are shown in Fig. 8. The area under the two curves was calculated numerically to calculate the total absorbance at the UV visible range, which is equal to the ratio between the two areas. The increase in the carbon content in the thin-film sample causes the two curves to be very close to each other, meaning that most of the solar radiation is absorbed by the sample [17].

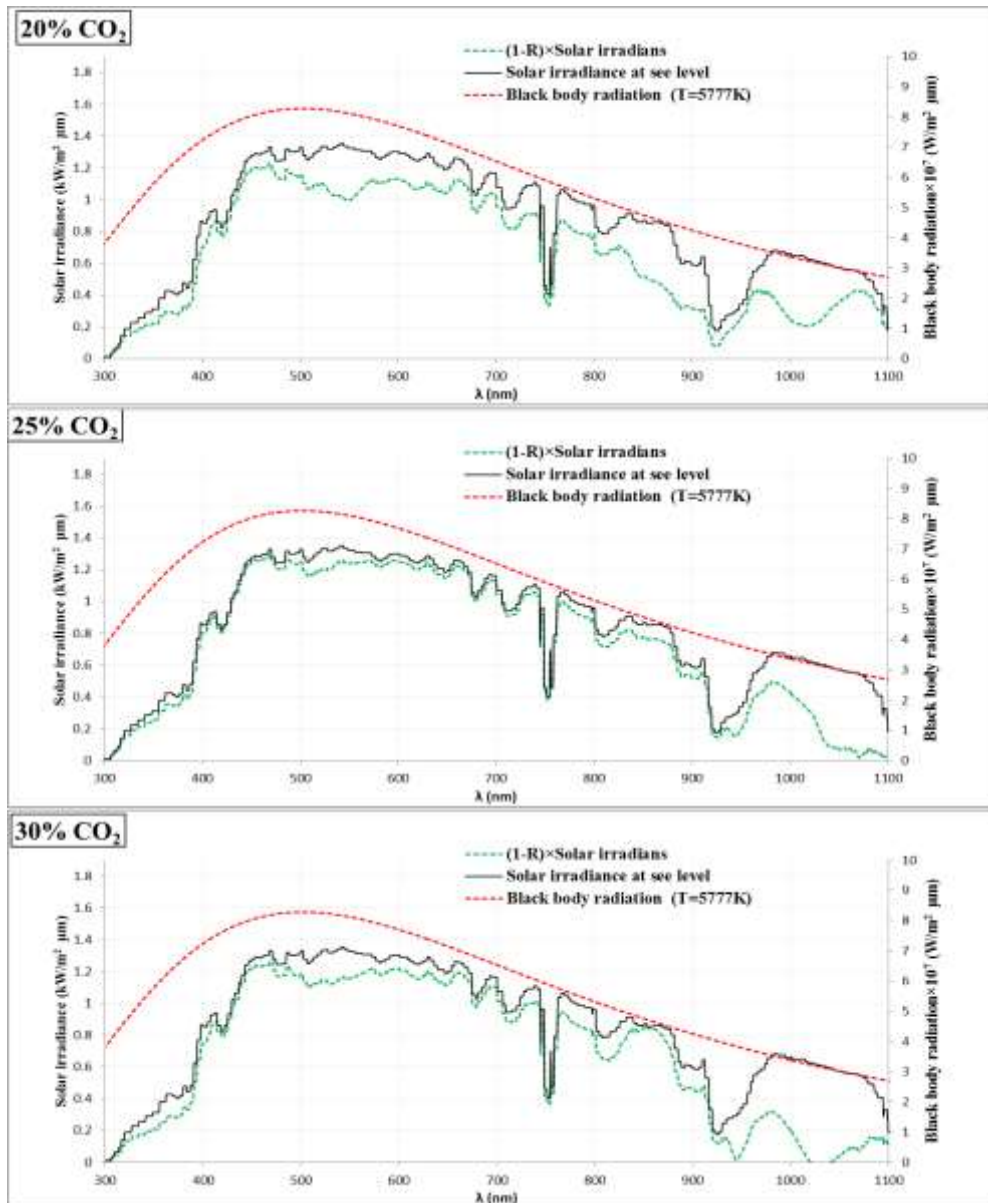


Figure 8-Comparison between solar irradiance curve and $(1-R) \times$ solar irradiance for copper substrate coated with CuO thin films prepared by DC sputtering at different CO_2 mixing ratios.

Figure 9 displays the black-body radiation curves at the operating temperature of the solar absorbers, proposed at 373 K, and the emission curves measured from the reflectance curve of the copper substrate coated by C: CuO thin-film prepared by DC sputtering using the three gas mixtures. The area under the two curves was numerically calculated to calculate the total emittance relative to the black body radiation in the infrared range. The area under the emittance curve was less than that of the sample deposited with reactive gas containing 25% carbon dioxide ratio.

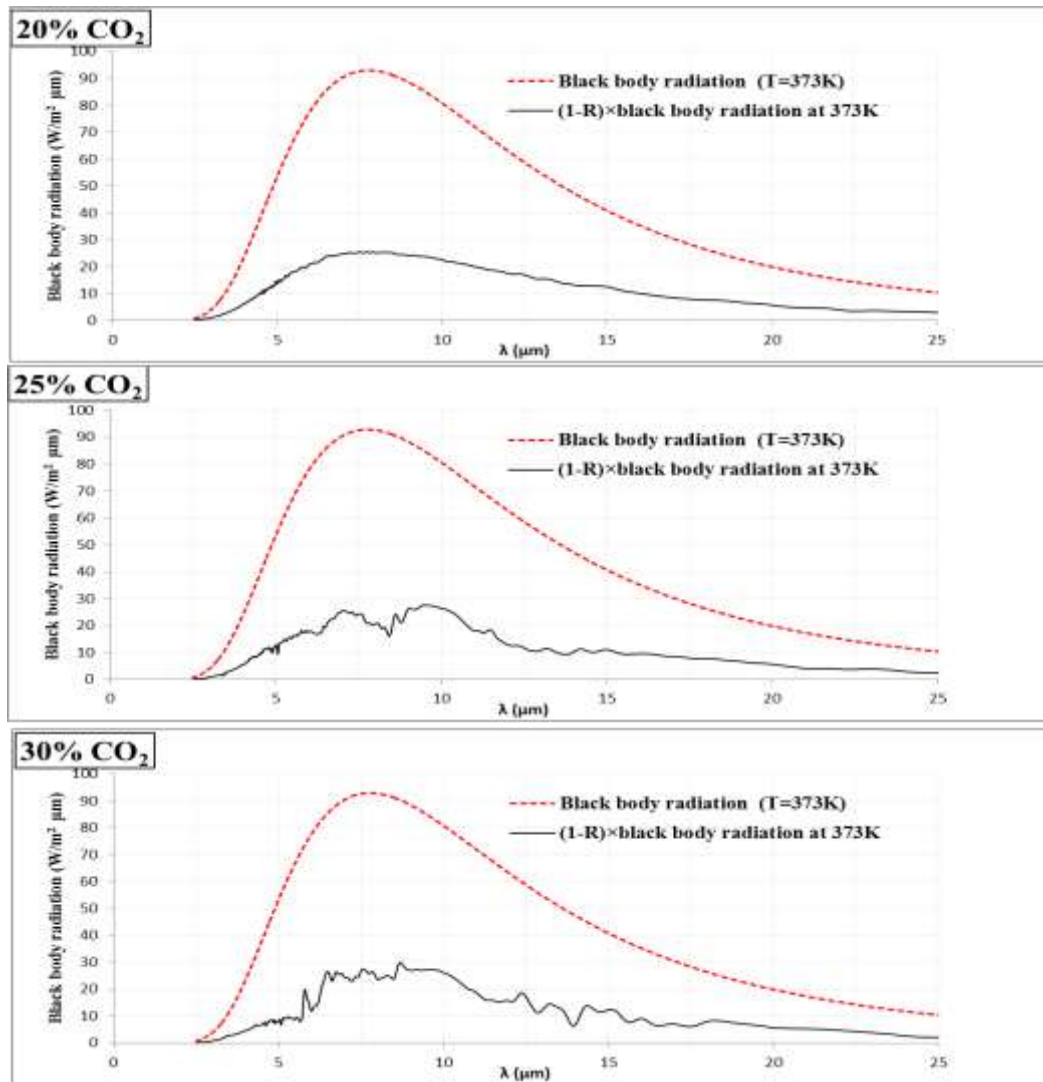


Figure 9- Comparison between black body radiation curve at 373 K and $(1-R) \times$ black body radiation for copper substrate coated with CuO thin films prepared by DC sputtering at different CO_2 mixing ratios.

Table 3 shows the UV-Visible absorptance and IR-emittance (at 373 K) for the copper substrates coated by Cu thin films prepared by DC sputtering using the three mixing ratios of the reactive gasses. It appears that the absorptance improved to 0.875 and the emittance reduced to 0.254 at 25 % CO_2 ratio of the reactive gasses. This result agrees with previous studies using different techniques [18].

Table 3-UV-absorptance and IR-emittance for the Cu substrate coated by CuO using different CO_2 mixing ratios

$\text{CO}_2\%$	α	ϵ
20	0.7873	0.276
25	0.8750	0.254
30	0.8106	0.259

4. Conclusion

A new selective absorber C-doped CuO coating of high quality was fabricated using reactive DC sputtering using a gas mixture of Ar, O_2 , and CO_2 at different ratios. The properties of the deposited thin films were tuned by varying the gas mixing ratios. Increasing the CO_2 ratio from 20 to 30% caused the increase of the carbon content of the deposited films; also the

crystalline size of carbon increased. Although the plasma density and plasma temperature were reduced by adding the reacting gases, due to the loss of plasma energy by secondary reactions, which in turn affects the sputtering efficiency, but adding limited proportions of the reacting gasses was effective in depositing films with good specifications, as its increase above a specific limit reduces the deposition efficiency. The best gas ratio, which produced the best sample as a selective absorber, was the 25% CO₂ reaction gas.

5. References

- [1] M. P. Pablo-Romero, R. Pozo-Barajas, and R. Yñiguez, "Global changes in residential energy consumption," *Energy Policy*, vol. 101, pp. 342–352, 2017.
- [2] L. Zhu, T. Ding, M. Gao, C. K. N. Peh, and G. W. Ho, "Shape Conformal and Thermal Insulative Organic Solar Absorber Sponge for Photothermal Water Evaporation and Thermoelectric Power Generation," *Adv. Energy Mater.*, vol. 9, no. 22, pp. 3–9, 2019.
- [3] K. Xu, M. Du, L. Hao, J. Mi, Q. Yu, and S. Li, "A review of high-temperature selective absorbing coatings for solar thermal applications," *J. Mater.*, vol. 6, no. 1, pp. 167–182, 2020.
- [4] B. Orel, H. Spreizer, L. S. Perse, M. Fira, A.Šurca Vuk, D. Merlini, M. Vodlan, M. Kohl, "Silicone-based thickness insensitive spectrally selective (TISS) paints as selective paint coatings for coloured solar absorbers (Part I)," *Sol. Energy Mater. Sol. Cells*, vol. 91, no. 2-3, pp. 93–107, 2007.
- [5] R. N. Abed, M. Abdallah, A. Adnan Rashad, H. Ch. Al-Mohammedawi, and E. Yousif, "Spectrally selective coating of nanoparticles (Co₃O₄:Cr₂O₃) incorporated in carbon to captivate solar energy," *Heat Transf. - Asian Res.*, vol. 49, no. 3, pp. 1386–1401, 2020.
- [6] J. R. Howell, R. Siegel, and M. P. Mengü, *Thermal radiation heat transfer*, 5th editio. New York: CRC Press, 2020.
- [7] G. K. Oster and R. A. Marcus, "Exploding Wire as a Light Source in Flash Photolysis," *J. Chem. Phys.*, vol. 27, no. 1, pp. 189–192, 1957.
- [8] M. Zhukov, *Plasma Diagnostics*, vol. 22, no. 1. Mosco: Lightning Source UK Ltd, 2005.
- [9] D. M. Devia, L. V Rodriguez-Restrepo, and E. Restrepo-Parra, "Methods Employed in Optical Emission Spectroscopy Analysis: a Review," *Ing. Cienc.*, vol. 11, no. 21, pp. 239–267, 2015.
- [10] S. S. Hamed, "Spectroscopic Determination of Excitation Premixed Laminar Flame," *Egypt. J. Solids*, vol. 28, no. 2, pp. 349–357, 2005.
- [11] N. M. Shaikh, S. Hafeez, B. Rashid, and M. A. Baig, "Spectroscopic studies of laser induced aluminum plasma using fundamental, second and third harmonics of a Nd: YAG laser," *Eur. Phys. Journal D*, vol. 44, pp. 371–379, 2007.
- [12] J. E. Sansonetti and W. C. Martin, "Handbook of Basic Atomic Spectroscopic Data," *Am. Inst. Phys.*, vol. 34, no. 4, 2005.
- [13] H. R. Humud and S. J. Kadhem, "Laser-Induced Modification of Ag and Cu Metal Nanoparticles Formed by Exploding Wire Technique in Liquid," *Iraqi J. Sci.*, vol. 56, no. 4B, pp. 3135–3140, 2015.
- [14] A. Lesage, "Experimental Stark Widths and Shifts for Spectral Lines of Neutral and Ionized Atoms," *J. Phys. Chem. Ref. Data*, vol. 19, no. 6, p. 1307, 2002.
- [15] H.R Humud, "Nonlinear Optical Properties of Pure and Ag/Polyaniline Nanocomposite Thin Films Deposited by Plasma Jet," *Iraqi J. Sci.*, vol. 57, no. 2C, pp. 1408–1414, 2016.
- [16] R. N. Abed, A. R. N. Abed, F. A. Khamas, M. Abdallah, and E. Yousif, "High performance thermal coating comprising (CuO:NiO) nanocomposite/c spectrally selective to absorb solar energy," *Prog. Color. Color. Coatings*, vol. 13, no. 4, pp. 275–284, 2020.
- [17] V. Teixeira, E. Sousa, M. F. Costa, C. Nunes, L. Rosa, M. J. Carvalho, M. Collares-Pereira, E. Roman, and J. Gago, "Spectrally selective composite coatings of Cr-Cr₂O₃ and Mo-Al₂O₃ for solar energy applications," *Thin Solid Films*, vol. 392, no. 2, pp. 320–326, 2001.
- [18] G. Katumba, A. Forbes, B. Mwakikunga, E. Wäckelgård, J. Lu, L. Olumekor, and G. Makiwa, "The Investigation of Carbon Nanoparticles Embedded In ZnO And NiO as Selective Solar Absorber Surfaces," in *Proceedings of ISES Solar World Congress*, 2007, pp. 551–555.